Electronic Supplementary Material (ESI) for Physical Chemistry Chemical Physics.

Polysulfide Induced Synthesis of Wide-layer-spacing MoS_2 Self-supporting Electrode for Efficient Electrocatalytic Water Splitting

Ningbo Yu ‡, Jianzhi Wang ‡, Hongliang Yu, Daichunzi Yang, Wentao Luo, Xiao Lin, Yanping Liu, Ning Cai, Yanan Xue and Faquan Yu *

Key Laboratory for Green Chemical Process of Ministry of Education, Hubei Key Laboratory for Novel Reactor and Green Chemistry Technology

Hubei Engineering Research Center for Advanced Fine Chemicals

School of Chemical Engineering and Pharmacy,

Wuhan Institute of Technology, Wuhan 430073, China

‡ These authors contributed equally to this work.

*Corresponding author:

Faquan Yu, Professor, PhD

Wuhan Institute of Technology

LiuFang Campus, No.206, Guanggu 1st road, Wuhan 430205, Hubei, China

E-mail address: fyu@wit.edu.cn

Tel: (86-27) 87194980; Fax: (86-27) 87194465

Materials

Molybdenum pentachloride ($MoCl_5$, AR), sublimed Sulfur (S, AR), sulfourea ($CS(NH_2)_2$, AR), 1,3-Diisopropenylbenzene (DIB, 99%), Nickel foam(NF, 99.8%), concentrated hydrochloric acid (HCl, 38%), potassium hydroxide (KOH, AR), N,N-Dimethylformamide(DMF, AR), Sodium Dihydrogen Phosphate (NaH_2PO_4, AR), Dibasic Sodium Phosphate(Na_2HPO_4, AR) and ethanol (C_2H_5OH, AR) were purchased from Sinopharm Chemical Reagent Co., Ltd. Commercial 20 wt.% Pt/C catalyst and commercial 20 wt.% RuO_2 catalyst were purchased from Shanghai Macklin Biochemical Co., Ltd. Nafion (5 wt.%) was purchased from Dupont China Holding Co., Ltd. All the chemical reagents were of analytical grade and were used as received without any purification. Water deionized with a Millipore system was used throughout

all experiments.

Preparation of polymeric sulfur

This polymeric sulfur (S-r-DIB) was prepared by ring opening polymerization via an inverse vulcanization technique. 0.089 g 1,3-Diisopropenylbenzene (DIB) was quickly added to 0.8 g molten sublimated sulfur at 185℃, stirred for a few minutes until the liquid is completely solidified, the S-r-DIB was obtained after cooling at room temperature.

Preparation of Pt/C and RuO_2 catalytic electrodes

4 mg commercial Pt/C (20 wt%) and 40 μL Nafion solution (5 wt%) were dispersed in the solution containing 640 μL DI water and 320 μL ethanol. After that, the mixture was ultrasonicated for 1 h. Subsequently, 500 μL of solution was dropwise onto the surface of freshly NF (0.5×0.5 cm^2), and then dried at room temperature.

The RuO_2 catalytic electrodes was obtained as the same as Pt/C catalytic electrodes, only changing Pt/C to RuO_2.

Materials characterization

X-ray diffraction (XRD) was carried out on a Shimadzu XRD-6100 with high-intensity Cu Kα radiation. Scanning electron microscopy (SEM) images were obtained by using Carl Zeiss Sigma-HD field-emission scanning electron microscope operated at 10 kV. X-ray photoelectron spectroscopy (XPS) measurements were conducted on Thermo Fischer ESCALAB 250Xi at 12.5 kV and 16 mA using an Al Kα X-ray source. Transmission electron microscope (TEM) images were collected on a JEOL JEM-ARF200F microscopy.

Electrochemical measurements

The electrochemical measurements data were obtained with a CHI760E electrochemical workstation (CH Instruments, China) in a typical three electrode system at room temperature. A mercuric oxide electrode, a graphite rod and a catalyst-loaded NF were used as reference, counter electrode and working electrode, respectively. For a typical HER measurement, linear sweep voltammetry (LSV) was obtained in a potential range from 0 to −0.5 V (vs RHE) with a sweep rate of 2 mV s^{-1} for 85% iR-compensation in N_2-saturated 1 M KOH (pH=14) electrolyte at room

temperature, as for OER measurement, it is the same as the HER test method, except that the interval is 1.2 to 1.9(vs RHE). Polarization curves for water splitting is collected at a scan rate of 5 mV s^{-1} after 85% iR compensation in a potential range from 1 to 2 V. The electrochemical active surface area (ECSA) voltammograms were carried out at various scan rates (20, 40, 60, 80 and 100 mV s^{-1}) at room temperature. The electrochemical impedance spectroscopy (EIS) was measured at the open circuit potential under an amplitude of 10 mV in a frequency range of 100 kHz to 0.01 Hz. The electrochemical stability of MoS_2/Ni_3S_2-p were tested using chronopotentiometry at a constant current density of −10 mA cm^{-2}, 100 mA cm^{-2} and 10 mA cm^{-2} for HER, OER and water splitting, respectively. Cyclic voltammetry (CV) measurements were 100 mV s^{-1} in −1.5 to 0.6 V.

Electrocatalytic performance calculations

ECSA can be obtained by the following equation [1]:

$$A_{ECSA} = \frac{C_{dl}}{C_s}$$

where "*Cs*" is the areal capacitance for a standard, and we employ the general value of 40 μF cm^{-2} for *Cs*.

TOF values of the electrochemical HER are calculated utilizing following equation [2]:

$$TOF = \frac{\text{hydrogen turnover number per area}}{\text{Mo atom numbers per area}}$$

$$= 5.18 \times 10 - 3 \times |J| \times \frac{Fw}{\text{loading mass}}$$

Here, where "*J*" is the current density at a specific applied potential (such as V vs. RHE = −0.2 V), The "Fw" in the equation correspond to the formula weight in MoS_2.

we have employed following equation to obtain the TOF values of the electrochemical OER [1]:

$$TOF = \frac{|J|S}{4nF}$$

Where the current density J at 1.60 V vs RHE is used for the estimation. "S" is the electrochemical surface area, "n" is the number of moles of active sites on the electrode surface (mol), "F" is Faraday constant (96485 C mol^{-1}) and "4" is the number of transferred electrons during the OER, and values of n can be calculated according to the formula:

$$n = \frac{Q}{2F} = \frac{I \times t}{2F} = \frac{I \times V/u}{2F}$$

Q is the cyclic voltammetric charge capacity obtained by integrating the CV cures, I is the current (A), V is the voltage (V) and u is the scanning rate (V s^{-1}).

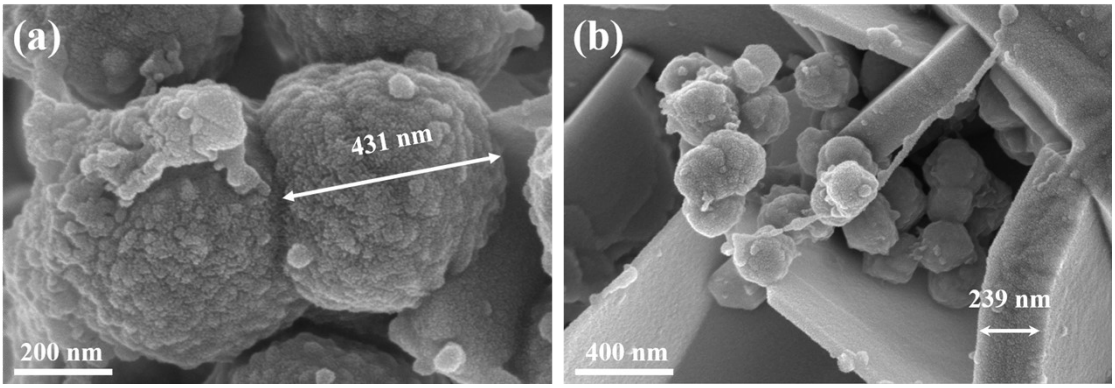

Fig. S1. The HRSEM images of MoS_2/Ni_3S_2-p

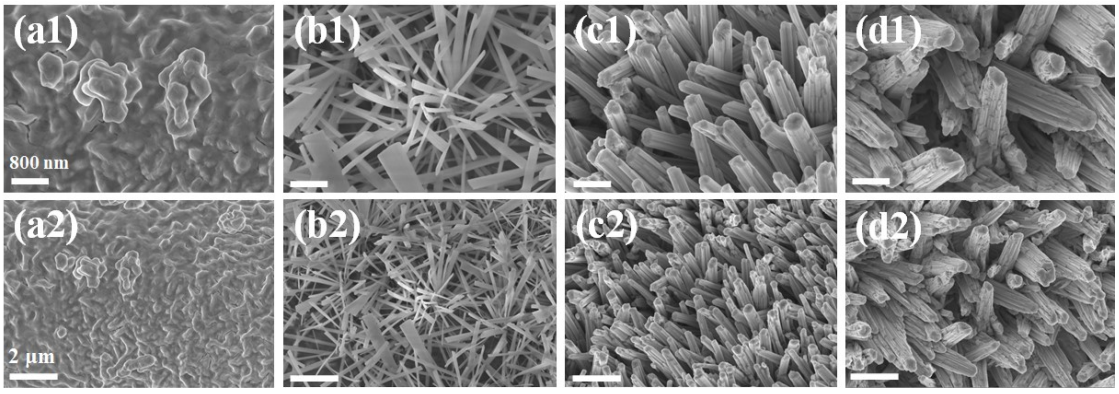

Fig. S2. The SEM images of (a) Mo, (b) MoS_2/Ni_3S_2-s, (c) MoS_2/Ni_3S_2-m and (d) Ni_3S_2.

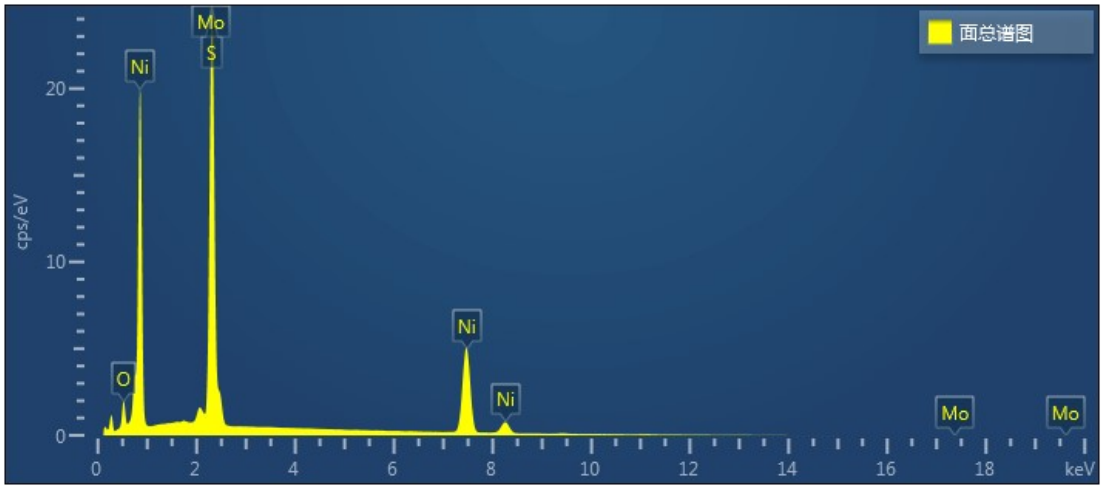

Fig. S3 The EDS spectrum of MoS_2/Ni_3S_2-p

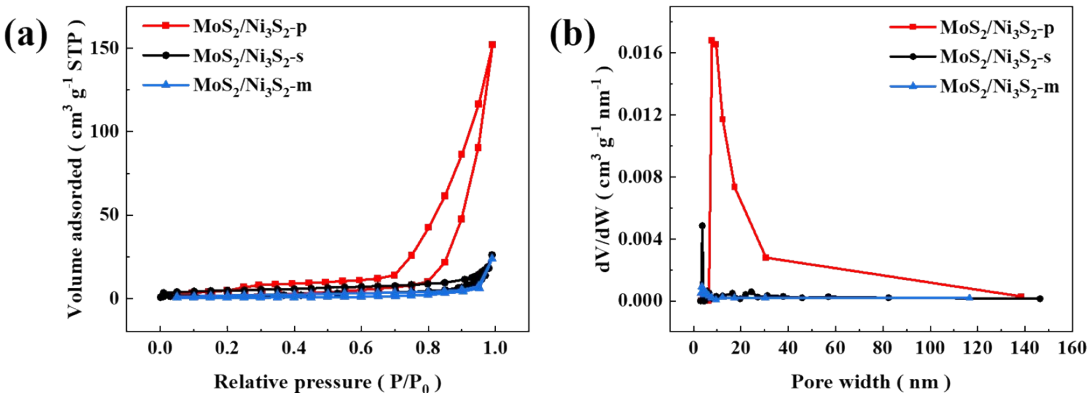

Fig. S4 (a) N_2 adsorption/desorption isotherms and (b) the corresponding Barrett-Joyner-Halenda (BJH) pore-size distribution curve determined from the desorption branch of the isotherm for MoS_2/Ni_3S_2-p, MoS_2/Ni_3S_2-s and MoS_2/Ni_3S_2-m.

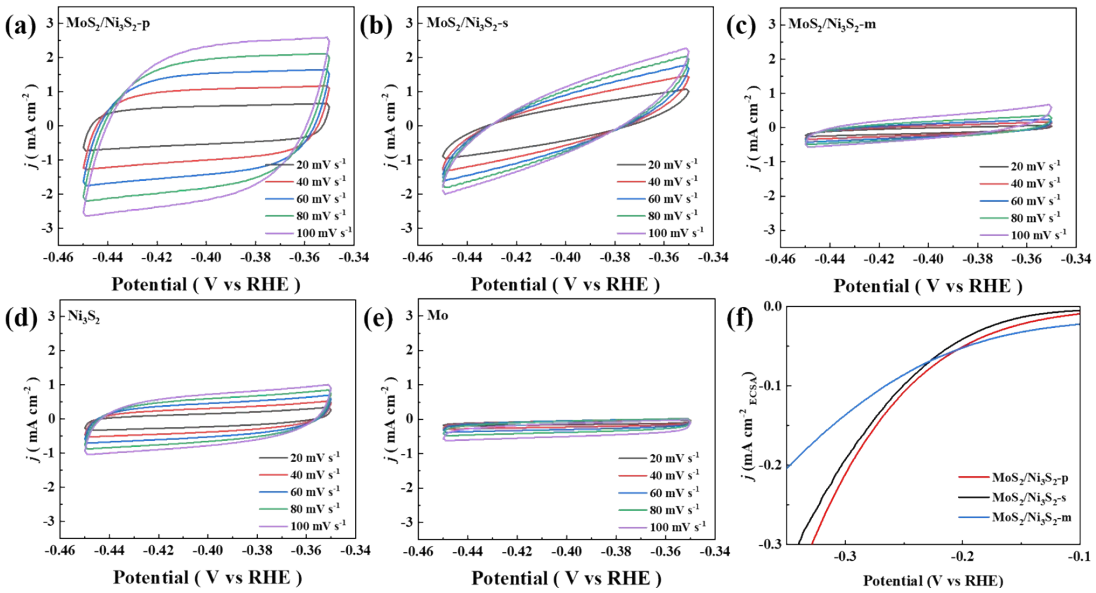

Fig. S5 Cyclic voltammograms toward HER of (a) MoS_2/Ni_3S_2-p, (b) MoS_2/Ni_3S_2-s, (c) MoS_2/Ni_3S_2-m (d) Ni_3S_2, (e) Mo, and (f) ESCA normalization.

Table S1 Comparison

Catalyst	Mass (mg)			Loading amount (mg cm^{-2})	TOF(s^{-1}) at -0.2 V per Mo atom
	start	end	differenc e		
MoS_2/Ni_3S_2-p	127.2	190.8	70.8	11.8	1.51
MoS_2/Ni_3S_2-s	131.1	222.3	91.2	15.2	0.41
MoS_2/Ni_3S_2-m	128.5	255.7	127.2	21.2	0.15

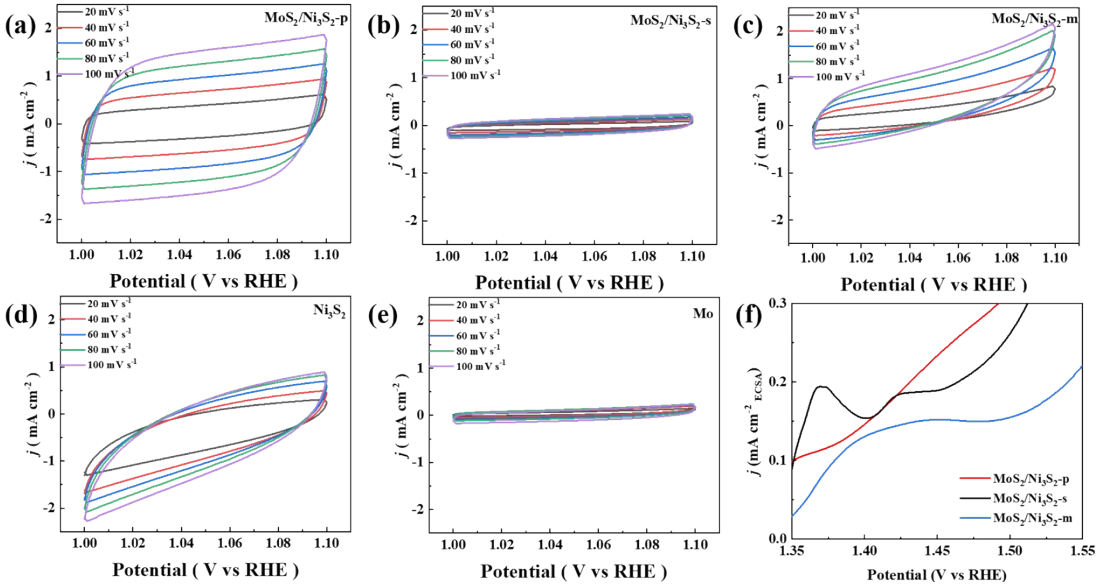

Fig. S6 Cyclic voltammograms toward OER of (a) MoS_2/Ni_3S_2-p, (b) MoS_2/Ni_3S_2-s, (c) MoS_2/Ni_3S_2-m (d) Ni_3S_2, (e) Mo and (f) ESCA normalization.

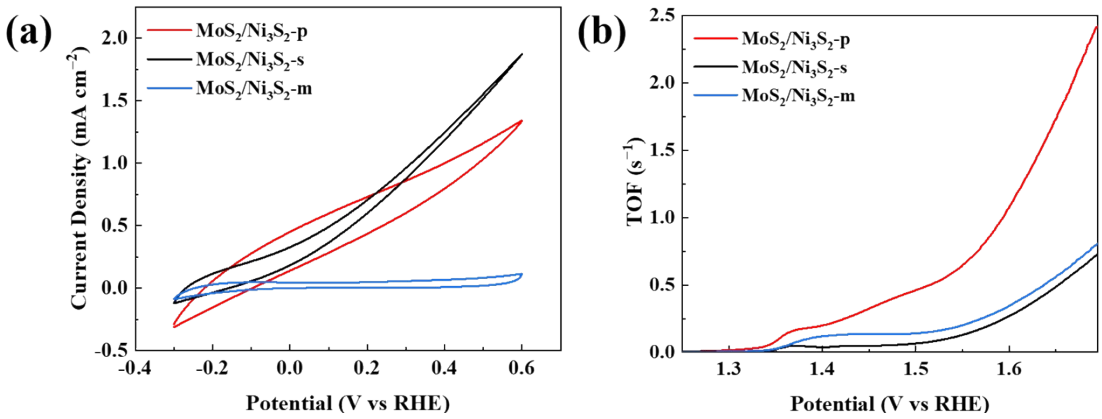

Fig. S7. (a) CV curves of MoS_2/Ni_3S_2-p, MoS_2/Ni_3S_2-s, MoS_2/Ni_3S_2-m in PBS solution (pH = 7.0) at a scan rate of 50 mV s^{-1}. (b) The TOFs of different catalysts.

Table S2 Comparison of the catalytic performance of MoS_2/Ni_3S_2-p with other previously reported electrocatalysts.

Catalysts	Electrolyte	Overpotential at -10 mA cm^{-2} for HER	Overpotential at 100 mA cm^{-2} for OER	Potential at 10 mA cm^{-2} for water splitting	Ref.
MoS_2/Ni_3S_2-p	1.0 M KOH	-145 mV	355 mV	1.55 V	This work
MoO_3/Ni–NiO	1.0 M KOH	-62 mV	347 mV	1.55 V	[3]
MoS_2@NiS_2	1.0 M KOH	-	356 mV	-	[4]
Co-MoS_2	1.0 M KOH	-56 mV	-	-	[5]
MoS_2/Ni_3S_2/NF	1.0 M KOH	-85 mV	-	-	[6]
Ni_3S_2/MoS_2	1.0 M KOH	-68 mV	-	-	[7]
MoS_2/Ni_3S_2	1.0 M KOH	-190 mV	-	-	[8]
MoS_2-MoO_{3-x}/Ni_3S_2	1.0 M KOH	-76 mV	-	-	[9]

References

[1] Xiao R, Huang P, Xiong T, et al. Advanced trifunctional electrodes for 1.5 V-based self-powered aqueous electrochemical energy devices[J]. Journal of Materials Chemistry A, 2023, 11(1): 374-384. DOI: 10.1039/d2ta05872c

[2] Huang Z, Luo W, Ma L, et al. Dimeric $[Mo_2S_{12}]^{2-}$ cluster: a molecular analogue of MoS_2 edges for superior hydrogen‐evolution electrocatalysis[J]. Angewandte chemie international edition, 2015, 54(50): 15181-15185. DOI: 10.1002/ange.201507529

[3] Li X, Wang Y, Wang J, et al. Sequential Electrodeposition of Bifunctional Catalytically Active Structures in MoO_3/Ni–NiO Composite Electrocatalysts for Selective Hydrogen and Oxygen Evolution[J]. Advanced Materials, 2020, 32(39): 2003414. DOI: 10.1002/adma.202003414.

[4] Wang X, Li L, Wang Z, et al. Construction of echinoids-like MoS_2@NiS_2 electrocatalyst for efficient and robust water oxidation[J]. Electrochimica Acta, 2020, 353:136527. DOI: 10.1016/j.electacta.2020.136527.

[5] Jin Q, Liu N, Dai C, et al. H_2-Directing Strategy on In Situ Synthesis of Co-MoS_2 with Highly Expanded Interlayer for Elegant HER Activity and its Mechanism[J]. Advanced Energy Materials, 2020, 10(20): 2000291. DOI: 10.1002/aenm.202000291.

[6] Xu H, Jiao Y, Li S, et al. Ultrathin-layered MoS_2 hollow nanospheres decorating Ni_3S_2 nanowires as high effective self-supporting electrode for hydrogen evolution reaction[J]. International Journal of Hydrogen Energy, 2020, 45(24): 13149-13162. DOI: 10.1016/j.ijhydene.2020.03.024.

[7] Feng J, Zhao Z, Tang R, et al. Interfacial Structural and Electronic Regulation of MoS_2 for Promoting Its Kinetics and Activity of Alkaline Hydrogen Evolution[J]. ACS Appl. Mater. Interfaces, 2021, 13(44): 53262–53270. DOI: 10.1021/acsami.1c17031.

[8] Narasimman R, Waldiya M, Jalaja K, et al. Self-standing, hybrid three-dimensional-porous MoS_2/Ni_3S_2 foam electrocatalyst for hydrogen evolution reaction in alkaline medium[J]. International Journal of Hydrogen Energy, 2021, 46(11): 7759-7771. DOI: 10.1016/j.ijhydene.2020.12.014.

[9] Luo M, Liu S, Zhu W, et al. An electrodeposited MoS_2-MoO_{3-x}/Ni_3S_2 heterostructure electrocatalyst for efficient alkaline hydrogen evolution[J]. Chemical Engineering Journal, 2022, 428: 131055. DOI: 10.1016/j.cej.2021.131055.